Available online at www.sciencedirect.com
ScienceDirect
Journal of Magnetic Resonance 191 (2008) 56–65
JMR Journal of Magnetic Resonance
www.elsevier.com/locate/jmr

Monte Carlo simulation of DNMR spectra of coupled spin systems

Zsófia Szalay, János Rohonczy *

Department of Inorganic Chemistry, Institute of Chemistry, Eötvös Loránd University, 112. Pf: 32, H-1518 Budapest, Hungary

Received 26 July 2007; revised 4 December 2007
Available online 8 December 2007

Abstract

A new program MC-DNMR is presented for the simulation of dynamic nuclear magnetic resonance spectra. The algorithm is a Monte Carlo type method based on the extension of single spin vector model to coupled spin systems. This extension is explained in detail and the theory is justified by examples. The main advantage of this program is the significantly smaller sizes of matrices than that in programs based on density matrix theory. So spectra of systems can be simulated that was impossible previously.

Keywords: DNMR; Dynamic NMR; Spectrum simulation; Monte Carlo method; Lineshape analysis

1. Introduction

Methods for direct simulation of dynamic NMR spectra are well-known for systems with chemical exchange [1–7]. The most widespread simulation programs (DNMR5 [8–11], MEXICO [12–14], WinDNMR [15,16], Bruker's TOPSPIN DNMR module [17]) are based on the calculation of transitions from the density matrix. The most important limitation of this method is the huge computer memory requirement even for simple spin systems. For example in a non-mutual exchange of three conformers, each containing three coupled spins (the number of spins is $N = 9$), the size of the 'supermatrix' to be diagonalized (without any simplification) would be $2^{4N} = 2^{36}$. This matrix blocks according to coherence level and these blocks are treated separately. The smaller blocks, the neglection of combinational transitions and the use of sparse matrix diagonalization methods [18,19] reduce the computer memory requirement radically, but the reduced matrix still can be too big for more complicated spin systems.

The huge memory requirement of DNMR spectra simulation (as compared to static spectra simulation) originates mainly from the fact that the dimension of the matrix to be diagonalized (with all possible simplifications mentioned above) is proportional to $s \cdot 2^{2n}$ where s is the number of sites of non-mutual exchanges and n is the number of spins in one conformer.

In this paper the theory and application of a new calculation method MC-DNMR is presented for 1/2 spin nuclei. The main advantage of it is that the required memory is much less in the case of 'multi-conformational' systems than the RAM requirement of the methods based on the calculation of density matrix. The reduction is achieved by separating kinetic and scalar coupling. This solves the problem mentioned above: the size of the calculated system is kept at the number of spins in *one* conformer (n) and the time dependency is handled statistically so the density matrix need not have to be calculated.

2. Theory

2.1. Monte Carlo simulation of dynamic behaviour

The description of the dynamic behaviour of the spin system in MC-DNMR program is based on the well-known vector model, where the *fid* is the result of the precession of net magnetisation vector. When an exchange occurs at time point t_{ex}, the Larmor frequency (ω) of the

* Corresponding author. Fax: +36 1 3722 909.
E-mail address: rohonczy@chem.elte.hu (J. Rohonczy).

1090-7807/$ - see front matter © 2007 Elsevier Inc. All rights reserved.
doi:10.1016/j.jmr.2007.12.002

vector alters but the momentary phase ($\Phi(t)$) of the vector remains unchanged, meaning:

$$\Phi(t) = \varphi_{\text{new}} + \omega_{\text{new}} \cdot t_{\text{ex}} = \varphi_{\text{old}} + \omega_{\text{old}} \cdot t_{\text{ex}}, \tag{1}$$

where φ_{old} and φ_{new} are the (initial) phases of the curves at $t = 0$. It means that after an exchange the initial phase of the new curve can be calculated as

$$\varphi_{\text{new}} = \varphi_{\text{old}} + (\omega_{\text{old}} - \omega_{\text{new}}) \cdot t_{\text{ex}}. \tag{2}$$

The *fid* is a continuous chain (to be called union) of the curves. After Fourier transformation the resulting spectrum has *a priori* statistical noise on it (Fig. 1), which can be decreased by averaging several scans (Monte Carlo method). This is in accordance with the fact that the sample contains several molecules and each of them has different dynamic behaviour; the spectra of the whole system can be simulated as the average of the spectra of individual molecules.

This model is described for single spin and two conformers in Ref. [3].

The time of the exchange is determined statistically based on the lifetime of the conformers. The (pseudo) first order kinetic equation for the concentration of conformer A_i is

$$\frac{\mathrm{d}[A_i]}{\mathrm{d}t} = \sum_{j \neq i} (-k_{ij}[A_i] + k_{ji}[A_j]), \tag{3}$$

where k_{ij} is the kinetic coefficient for the reaction

$$A_i \rightarrow A_j. \tag{4}$$

At the start of the detection the actual conformation of the molecule is determined using a random number and the equilibrium composition. The latter can be calculated from Eq. (3) assuming equilibrium (all derivatives are zero).

According to Eq. (3) the kinetic coefficient for the decay (d_i) of the component A_i is

$$d_i = \sum_{j=1}^{m} k_{ij}. \tag{5}$$

where m is the number of conformers and $k_{ii} = 0$. The probability ($V^i_{\Delta t}$) of the event that the molecule is remaining in the same A_i conformation for a time period of Δt is:

$$V^i_{\Delta t} = \exp(-d_i \cdot \Delta t), \tag{6}$$

meaning that the length of each time period is given by an exponential distribution. Therefore the moment of the exchange (t_{r+1}) of a molecule can be given as

$$t_{r+1} = t_r - \ln(\text{rnd})/d_i, \tag{7}$$

where t_r is the time of the previous exchange and rnd is a random number with uniform distribution between 0 and 1. The period between t_r and t_{r+1} (when no exchange occurs) is the time slice r.

If more than two conformers are present in the system ($m > 2$), the conformer in time slice $r + 1$ is determined statistically using the ratio of the kinetic coefficients (k_{ij}).

In the program the kinetic coefficients are calculated from the activation parameters using the Eyring–Polányi equation

$$k = \frac{\kappa \cdot k_B}{h} \cdot T \cdot \exp\left(-\frac{\Delta H^{++} - T\Delta S^{++}}{RT}\right). \tag{8}$$

where h, k_B and R are the Planck, Boltzmann and the universal gas constants, κ is the transmission coefficient, ΔH^{++} and ΔS^{++} are the activation enthalpy and entropy of the reaction and T is the temperature.

2.2. Extension of single spin vector model

The model described above relies on the vector model and the behaviour of net magnetisation vector. In the case of a single spin without chemical exchange this vector is precessing with one frequency resulting in a sine function

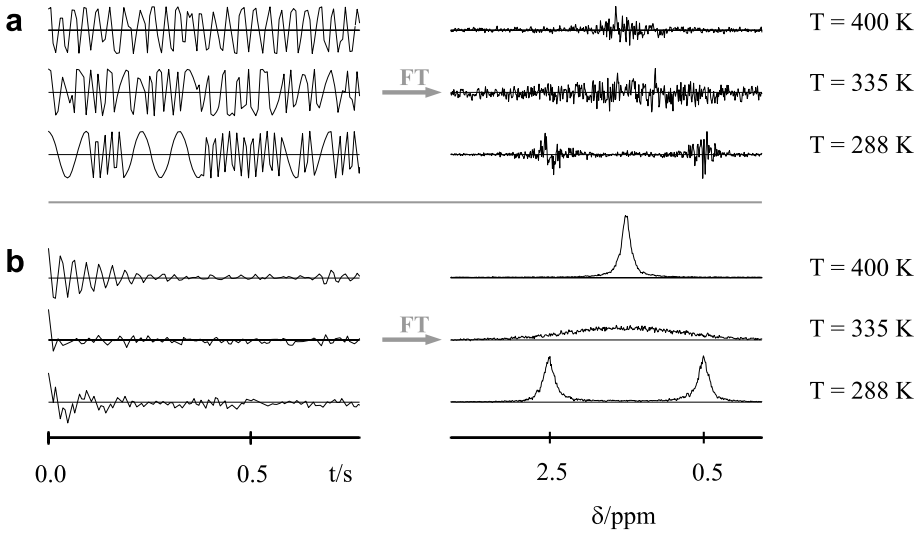

Fig. 1. The effect of the number of scans and temperature using Monte Carlo simulation of DNMR spectra for a single spin. (a) 1 scan, (b) 100 scans.

as *fid* (if relaxation is neglected). In coupled spin systems the *fid* is the sum of several sine functions according to the several single quantum coherences and the several energy levels. These energy levels can be determined from the Hamiltonian in angular frequency units [3]:

$$\hat{H} = 2\pi \sum_i \nu_i \hat{I}_{zi} + 2\pi \sum_i \sum_{i<j} J_{ij} \hat{I}_i \hat{I}_j, \tag{9}$$

where ν_i is the chemical shift of spin i (in Hz), J_{ij} is the coupling constant between nuclei i and j. The differences of the eigenvalues give the frequencies of the sine functions.

The dynamic spectrum could be simulated if the sine functions of any two conformers could be paired systematically. The problem is that they cannot be, since the eigenfunctions—needed for systematic pairing—are lost during an exchange. Therefore the exchange should be handled statistically: each function can change into any sine of the new state. So the problem leads to the determination of the probability of a given eigenfunction changing into an other.

The second criterion is that the phase of the precessing vector must be continuous at the moment of an exchange. But the new phase cannot be calculated as easily as for a single spin because the eigenfunction itself alters during the exchange. The basis functions ($\alpha\alpha\ldots\alpha$, $\alpha\alpha\ldots\beta$,..., $\beta\beta\ldots\beta$) are the ones those are keeping their phases in a reaction. These vectors are independent of molecular conformations and only their speed will change during exchanges. The problem is that basis functions are not eigenfunctions of the Hamiltonian in a coupled spin system and they do not have well defined energy, therefore the speed of the vectors can only be determined as the probability distribution of well defined frequencies. To determine these frequencies and probabilities we first determine the energy distribution of the basis states.

The energy levels of the extended model for the case of a strongly coupled AB system are shown on Fig. 2. In an uncoupled or weakly coupled spin system the four basis functions represent the eigenfunctions of the system. In this case basis functions have exact energies (Fig. 2b). The strong coupling combines the basis functions (e.g. Φ_2 and Φ_3 on Fig. 2) into eigenfunctions. In this case only the eigenfunctions have well-defined energies. Each basis state is characterized by a set of energy levels (the eigenvalues of the Hamiltonian). Mathematically the uth eigenvector (Ψ_u) of a coupled spin system is linear combination of the basis vectors (Φ_f) with c_{uf} coefficients, where f is the index of the basis functions

$$\Psi_u = \sum_f c_{uf} \Phi_f. \tag{10}$$

The matrix of the c_{uf} coefficients is real and unitary, therefore each basis function can be expressed easily on the basis of the eigenfunctions as

$$\Phi_f = \sum_u c_{uf} \Psi_u. \tag{11}$$

This splitting of the energy levels is similar to the one in LCAO–MO method (Fig. 3). The independent basis functions (LCAO: atomic orbitals) are interacting and because of the coupling (LCAO: overlapping) they are combined to eigenfunctions (molecule orbitals) and the energies of these

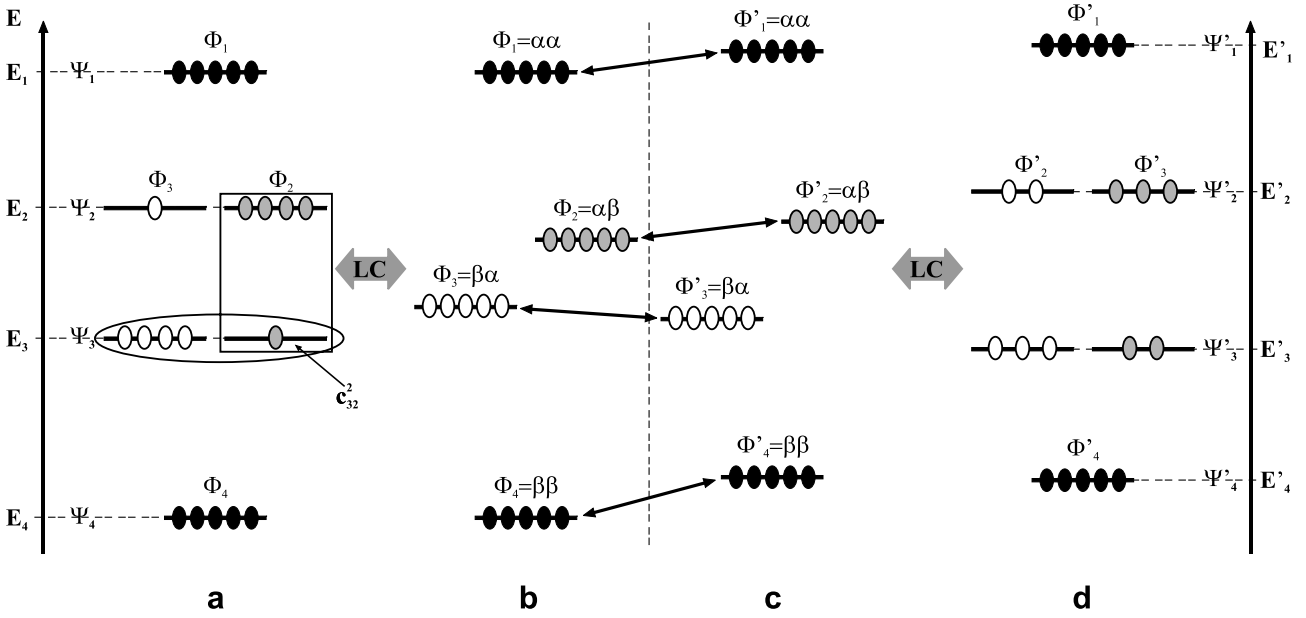

Fig. 2. Extension of the vector model to coupled spin systems: energy levels and populations of an AB spin system. (a) Perturbed energy levels of the coupled system. Because of coupling, energy levels of basis states split into eigenstates (as linear combinations, LC) with well-defined energies. The population of each energy level is given by LC coefficients. On the figure the states inside the rectangle are in basis state Φ_2 and the ones in the ellipsoid are in eigenstate Ψ_3. (b) Basis states of the spin system. Expectation values (energy) are calculated without higher order coupling. (c) Unperturbed energy levels after an exchange reaction. (d) After the exchange energy levels are still strongly coupled with new LC coefficients and populations.

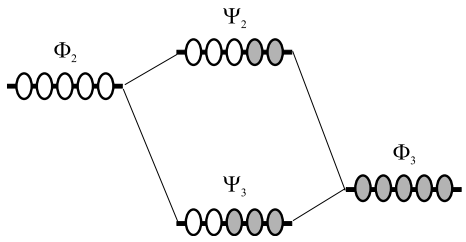

Fig. 3. Splitting of energy levels. Calculation method is similar to the one used in LCAO–MO theory.

ones give the energy levels of the spin system. The population or probability of the new energy levels (in a given basis state) is given by the corresponding linear combination coefficients. If one molecule is in basis state Φ_f, the probability of being at eigenstate Ψ_u is c_{uf}^2 (c_{32}^2 on Fig. 2a). As the eigenfunctions with different total spin quantum numbers are independent, the probability of frequency ω_p (meaning the frequency of $\Psi_u \rightarrow \Psi_v$ transition) in basis state pair $\Phi_g \rightarrow \Phi_f$ is

$$P_{pe} = P_{uvfg} = c_{uf}^2 \cdot c_{vg}^2, \tag{12}$$

where p denotes the eigentransition (uv pair) and e denotes the basis function pair (f and g). For a coupled spin system this means that the energy of a given basis state can be expressed as the set of eigenvalues with their specified probabilities.

2.3. Mathematical formalism

As it was shown in the previous section the basis transitions of a coupled spin system can be described as the linear combination of the eigentransitions and they have discrete frequency distributions. For example in the case of a classic AB spin system the mixed transition $\alpha\beta \rightarrow \alpha\alpha$ ($e = 0$)—as a combination of two eigentransitions—has two frequencies (ω_p, $p = 1$ or 2). Before the exchange the *fid* of such a transition is the sum of two sine functions (written in complex exponential form) (Fig. 4a)

$$fid(t) = I_1 \exp(\mathrm{i}\omega_1 t) + I_2 \exp(i\omega_2 t). \tag{13}$$

The intensity of each curve (I_p) is given as the product of its probability ($P_p = P_{0p}$ from Eq. (12)) and its amplitude (a_p):

$$I_p = P_p a_p, \tag{14}$$

where a_p amplitudes of the eigentransitions are determined from the linear combination coefficients in Eq. (10) as matrix elements of I^+ operator:

$$a_p = a_{uv} = |\langle \Psi_u | I^+ | \Psi_v \rangle|^2 = \left| \sum_f c_{uf} c_{vf} \right|^2. \tag{15}$$

After the exchange (at time point t_{ex}) each curve continues in two new sine functions with $q = 1, 2$ (q is the index of the 'new' eigentransition) with intensities $I_{pq} = P_p P_q a_q$, as the

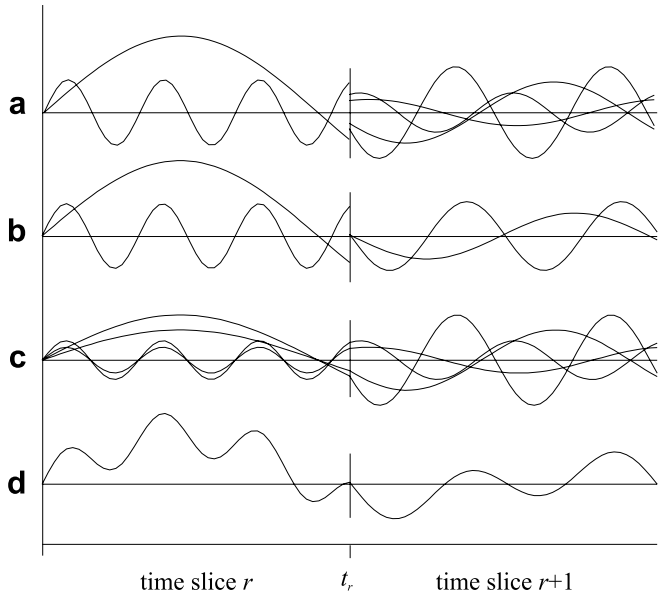

Fig. 4. Calculation of *fid* before and after an exchange. (a) Exponential growth after each exchange due to splitting of each curve. (b) Curves calculated with the simplification described in the text. (c) Curves of each pairing proving that the phase is actually continuous. (d) The overall *fid*.

frequencies of the basis transition (ω_p and ω_q) are independent from each other. This results in four new curves:

$$f(t) = \sum_{q=1}^{2} \sum_{p=1}^{2} I_{pq} \exp(\mathrm{i}(\omega'_q t + \varphi_{pq})), \tag{16}$$

where t is the time elapsed since the start of detection ($f(t)$ is valid only for $t > t_{ex}$).

If the duplication of the curves would continue after each exchange, it would lead to unmanageable amount of calculations (Fig. 4a). After the exchange there are sine functions with the same frequencies and their sum can be expressed as a sine with their common frequency:

$$f(t) = \sum_{q=1}^{2} \left[\left(\sum_{p=1}^{2} I_{pq} \exp(\mathrm{i}\varphi_{pq}) \right) \exp(\mathrm{i}\omega'_q t) \right]. \tag{17}$$

Simultaneously, the phase and the intensity (to be called phase factor—y) of each replacing sine must be recalculated

$$y'_q = I'_q \exp(\mathrm{i}\varphi'_q) = \sum_{p=1}^{2} I_{pq} \exp(\mathrm{i}\varphi_{pq}). \tag{18}$$

resulting in the expression

$$f(t) = \sum_{q=1}^{2} I'_q \exp(\mathrm{i}(\omega'_q t + \varphi'_q)). \tag{19}$$

Eq. (19) means that only two frequencies remain in each time slice (Fig. 4b). This simplification prevents the exponential growth of the number of curves.

Apparently, we seem to loose the continuity of the phases on Fig. 4b but that is only true for the parts of

the *fid*. Focusing only on one molecule pair its basis state has only one frequency and its *fid* is proportional to one of the (continuous) curves on Fig 4c. In a time slice the curves with the same frequency can be handled together. The continuity of their sum breaks because of different grouping but the total *fid* is continuous again as shown on Fig. 4d.

In other words the *fid* of one conformer is the sum of two precessing vectors. These vectors have different length and amplitude but their total length is constant. After an exchange each vector is divided into two other ones having ω'_1 and ω'_2 frequencies. The vectors those are precessing with the same frequency can be added and be handled together, so only two vectors remain again. The details of this method are shown on Fig. 5. The process starts at A, the two vectors precess until the point of exchange (B) giving the first two curves on Fig. 4b. At that point each vector is divided according to the new frequency distribution and vectors of same frequencies are added to each other (C). This gives the same result as if the two vectors were added to each other and then the sum was split according to the given distribution. The remaining two vectors (D) start precession from common phase with different frequencies (E) giving the other two sine curves on Fig. 4b. Cycle B–E continues until the end of acquisition time.

As a general, the *fid* of a base pair between two exchanges (t_r and t_{r+1}) without relaxation is

$$\begin{aligned} fid_{r+1}(t) &= y_p^{r+1}\exp(\mathrm{i}\omega_p^{r+1}t) \\ &= \sum_p \sum_q (a_p P_{pe} y_q^r \exp(\mathrm{i}(\omega_p^{r+1}t + \varphi_{pq}^r))), \end{aligned} \tag{20}$$

and the frequency-dependent complex phase correction y_q^r can be calculated recursively as

$$\begin{aligned} y_p^{r+1} &= a_p P_{pe} \sum_q y_q^r \exp(\mathrm{i}\varphi_{pq}^r) \\ &= a_p P_{pe} \sum_q y_q^r \exp(\mathrm{i}(\omega_q^{r+1} - \omega_p^r)t_r), \end{aligned} \tag{21}$$

where r is the index of the time slice, t_r is the same as before, p and q are the indices of transitions in time slices $r+1$ and r, respectively, a_p is the amplitude and P_{pe} is the probability of transition p (the latter depends on the actual basis transition e as well), ω_p^{r+1} (and ω_q^r) is the frequency of transition p (and q) in time slice $r+1$ (and r) and φ_{pq}^r is the new phase of the transition p if the previous transition was q.

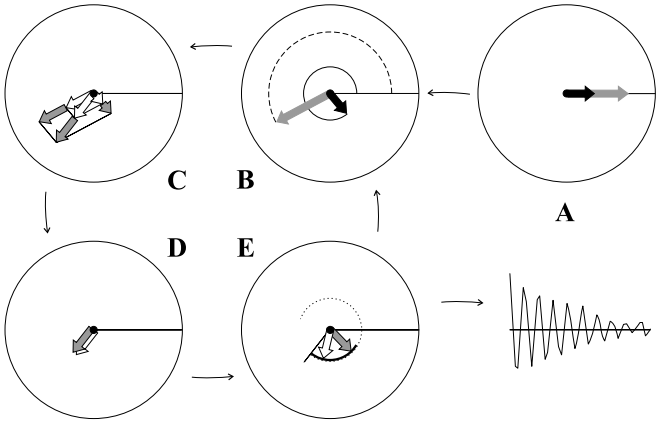

Fig. 5. The calculation algorithm in the vector model.

Eq. (20) results in a simpler expression after grouping by frequency (ω_p^{r+1})

$$fid_{r+1}(t) = y_r \sum_p P_{pe} a_p \exp(\mathrm{i}\omega_p^{r+1}(t - t_r)), \tag{22}$$

The phase factor (y_r) is independent of the frequency ω_p^{r+1} and shows the remaining magnetisation vector at t_r (step C on Fig. 3). It can be calculated recursively as

$$y_{r+1} = y_r \sum_p P_{pe} \exp(\mathrm{i}\omega_p^{r+1}(t_{r+1} - t_r)). \tag{23}$$

From Eqs. (22) and (23) the $Y(\omega)$ spectrum can be calculated after multiplying them with the exponential term (the relaxation with T^* time constant) and performing Fourier transformation

$$\begin{aligned} Y_{r+1}(\omega) = \frac{1}{t_{r+1} - t_r} \int_{t_r}^{t_{r+1}} & y_r \sum_p P_{pe} a_p \exp(\mathrm{i}\omega_p^{r+1}(t - t_r)) \\ & \times \exp\left(-\frac{t}{T^*}\right) \exp(-\mathrm{i}\omega t)\mathrm{d}t. \end{aligned} \tag{24}$$

This equation—after integration and denoting $(t_{r+1} - t_r)$ as Δt_r and $(\omega_p^{r+1} - \omega)$ as $\Delta\omega_p$—leads to

$$\begin{aligned} Y_{r+1}(\omega) = y_r & \frac{\exp((\mathrm{i}\omega - T^{*-1})t_r)}{\Delta t_r} \\ & \times \sum_p a_p P_{pe} \frac{T^{*-1} + i\Delta\omega_p}{T^{*-2} + (\Delta\omega_p)^2} \\ & \times (1 - \exp((\mathrm{i}\cdot\Delta\omega_p - T^{*-1})\Delta t_r)). \end{aligned} \tag{25}$$

This should be summarized for each time slice (r), scan (s) and base pair (e) and the calculated spectrum is the real part of the following curve:

$$\begin{aligned} Y(\omega) = \sum_e \sum_s \sum_r \Bigg[& y_r \frac{\exp((\mathrm{i}\omega - T^{*-1})t_r)}{\Delta t_r} \sum_p a_p P_{pe} \\ & \times \frac{T^{*-1} + i\Delta\omega_p}{T^{*-2} + (\Delta\omega_p)^2} \left(1 - \exp\left((\mathrm{i}\Delta\omega_p - T^{*-1})\Delta t_r\right)\right) \Bigg]. \end{aligned} \tag{26}$$

This algorithm requires lots of time because of a rather complicated calculation to be done for each (e, s, r) triplet at each frequency. To avoid this problem the discrete *fid* can be expressed as the union ($\bigcup$) of the *fid*s in the time slices (r) and added for each scan (s) and each basis pair (e) which finally leads to the expression

$$\begin{aligned} fid(t) &= \sum_s \sum_e \bigcup_r fid_{r+1}(t) \\ &= \sum_s \sum_e \bigcup_r y_r \sum_p P_{pe} a_p \exp(\mathrm{i}\omega_p^{r+1}(t - t_r)). \end{aligned} \tag{27}$$

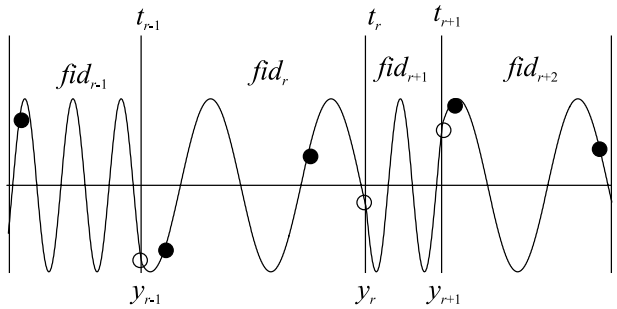

Fig. 6. Calculation algorithm of the MC-DNMR program. The fid points (●) are calculated in the time slice they appear and the phase factor (y) is calculated at the exchange point (○) ending the time slice. If there is no fid point in a time slice between t_r and t_{r+1} than only the phase factor y_{r+1} is calculated.

After that discrete Fourier transformation is performed to get the simulated temperature dependent spectrum.

The importance of Eq. (27) is that it gives the *fid* as a continuous curve in time. By discrete sampling only a few thousand points (e.g. TD) of this curve are calculated. If the rates of exchange are so fast, that there are more than one exchange points between two sampling points (see t_r and t_{r+1} on Fig. 6), there are time slices without sampling point. In the case of such 'dummy' slices only phase factors (y) are calculated at the end of these time slices. Practically it means that there is no upper limit for the reaction rate; time slices can be shorter than the dwell time and then there are empty sets in the union of data points.

3. Program properties

The algorithm of the MC-DNMR program is based on the theoretical background explained above. It was written in the platform independent Java programming language.

Input parameters:

- Spectrum parameters (spectrum width and offset, resolution, acquisition and relaxation time).
- Simulation parameters (number of scans, temperatures, nuclei and conformers).
- Spin system parameters (chemical shift values and scalar coupling constants for each conformer).
- Chemical exchange parameters (activation enthalpies and entropies, temperature data).

The results and optional results can be the followings:

- The calculated spectra or *fid*s.
- Eigenvectors and eigenvalues of the static Hamiltonian and the intensities of the transitions (may be used in other simulations).
- In the case of aborted calculation a temporary output. Further calculation can be continued from these data.

Constraints (including RAM and time):

- Typical values are 100–1000 scans, 1–16 nuclei per conformer (maximum depends on RAM and time). There is no upper limit for the number of conformers and that of temperatures.
- The exchange reactions between conformers can be mutual or non-mutual, but always with (pseudo) first order kinetics.
- All nuclei are of 1/2 spin.
- There is no scalar coupling between the exchanging sites (e.g. mutual exchange of an AB system cannot be simulated).

The reason of the last constraint is that the theory of the whole program relies on the separation of scalar coupled spin systems which are connected to each other through chemical exchange reactions but J-coupling is not allowed between the separated systems. The mutually exchanging AB spin system, which is very common example in the literature, violates this restriction and its simulation yields doublet instead of a singlet at high temperature which is a non-realistic result.

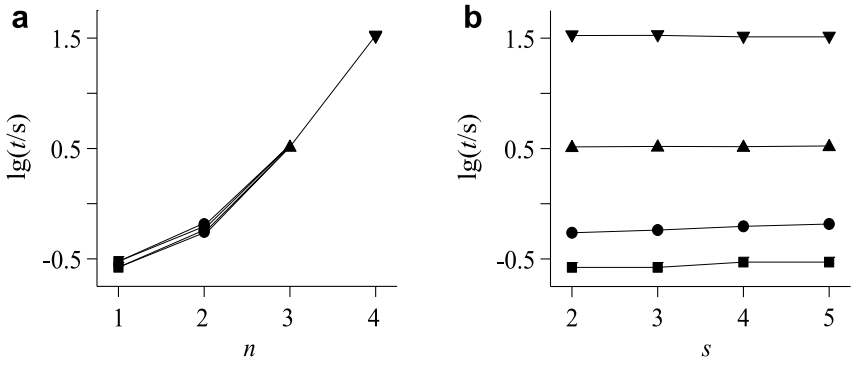

Fig. 7. Runtime as a function of (a) the size of the spin system (n) and (b) the number of exchanging sites (s). Four series (■, ●, ▲ and ▼) were calculated with uncoupled ($n = 1$) and strongly coupled spin systems ($n = 2$, 3 and 4 nuclei). Other common parameters: $k = 40\ s^{-1}$, NS = 100 scans.

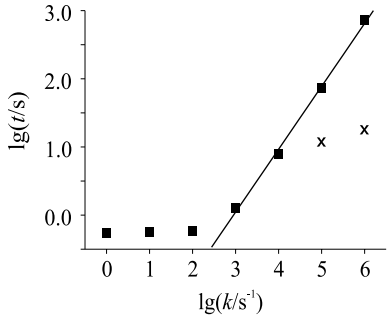

Fig. 8. Runtime vs. rate constant (k) of exchange reactions. Two series were calculated with NS = 100 (■) and with variable NS providing constant signal to noise (×). Generally above the coalescence temperature less scans are enough to achieve the same S/N ratio. Model: non-mutual two-site exchange of a coupled AB spin system.

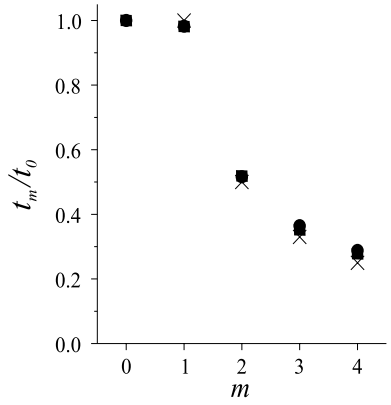

Fig. 9. The effect of multiple program threads (m) on normalized runtime $t_m/t_0.t_m$ is the runtime of m threads and t_0 means the runtime of the program without multithreading. Model: two site non-mutual exchange of an AB spin system, $k = 400\ s^{-1}$, NS = 1000 scans (●), $k = 4000\ s^{-1}$, NS = 10,000 scans (■) and theoretical ($1/m$) values (×).

Our algorithm requires much less RAM than the ones calculating density matrix. The coefficient matrices are real, and the dimension of the largest one is $\binom{n}{n/2} \sim 2^n$ for n nuclei whereas in the density matrix method the matrices are complex and the largest one is of dimension $s \cdot \binom{n}{n/2} \cdot \binom{n}{n/2+1} \sim s \cdot 4^n$ where s is the number of exchanging sites.

The runtime of the program is a more complicated matter. The program calculates the *fid*s of all the $\binom{2n}{n-1}$ basis transitions separately which means that the runtime increases exponentially with the size of the spin system (n). On the other hand, runtime is practically independent of the number of exchanging sites (Fig. 7).

Besides the number of conformers and nuclei, the runtime also depends on the number of exchanges during the acquisition because phase factors (y in Eqs. (22)–(27)) must be calculated at the end of each time slice even at the end of 'dummy' ones (Fig. 8). This means that for fast reactions the runtime is proportional to the reaction rates (k) if the same number of scans is calculated. In the meantime the signal to noise ratio improves faster above coalescence than below, therefore spectrum with the same quality can be calculated from less scans. This means that calculation time does not increase linearly with k.

For spin systems with more than three or four nuclei the runtime can exceed days. One advantage of this Monte Carlo method is that the time consuming calculation can be easily parallelised using dozens or hundreds of program threads or processors. The calculation of the terms of the outmost sum in Eq. (27) can be separated into independent threads running the same algorithm. This separation is

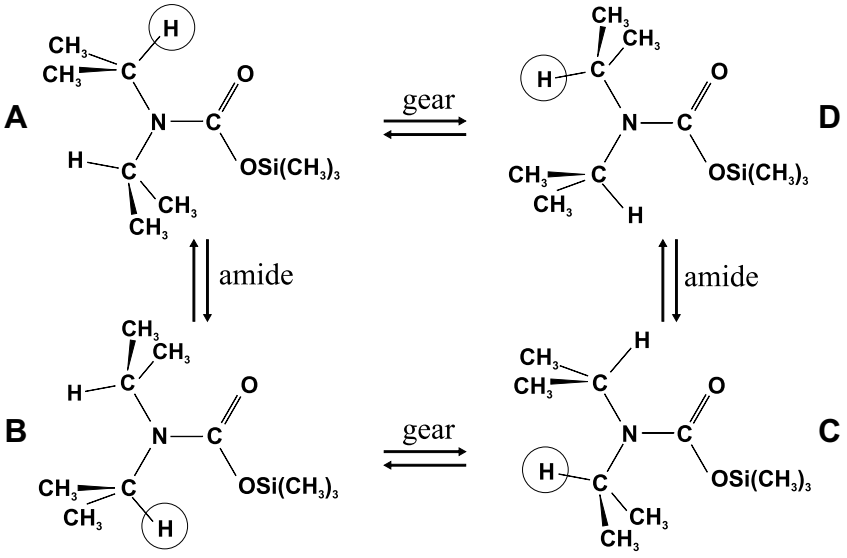

Fig. 10. Structure and exchange reactions of *N,N*-diisopropyl carbamic acid trimethyl silyl ester (^{i}PrSiC).

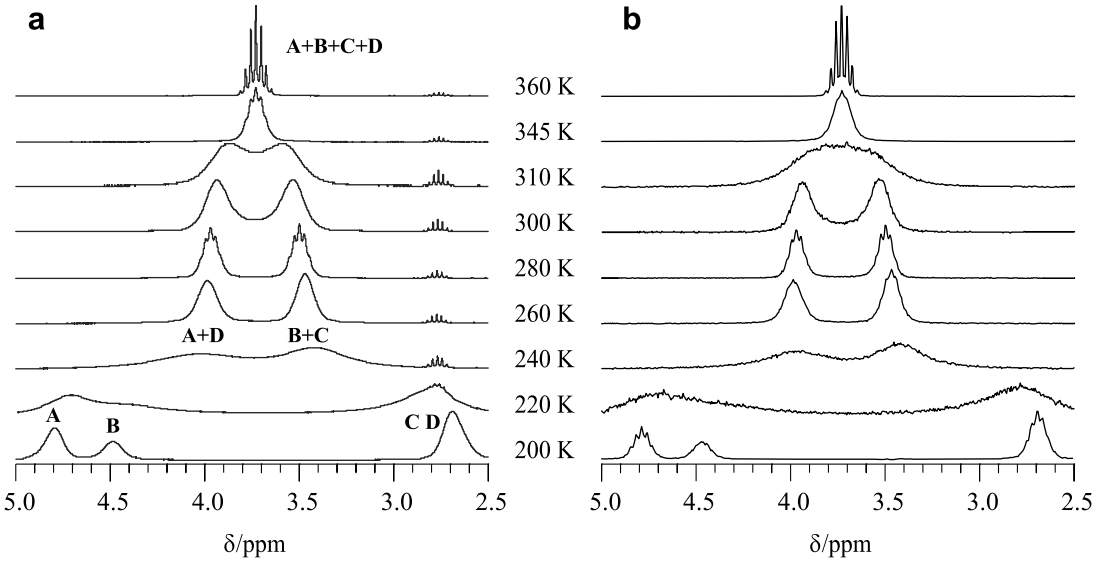

Fig. 11. ^{i}Pr-methine part of the ^{1}H NMR spectrum of ^{i}PrSiC at different temperatures: (a) Experimental (b) calculated. The simulation of the spectra (SI = 512, NS = 100 scans) with MC-DNMR program was performed with 16 Java threads on four nodes of an FSC Primergy RX220 Rack Server at HPC-Szeged, each node with two 1.8 GHz AMD Opteron dual-core processors. The computation times were 1 min, 1.3 min, 3 min, 12.5 min, 1.25 h, 4 h and 7.5 h, for $T = 200$, 220, 240, 260, 280, 300 and 310 K, respectively. At $T = 345$ and 360 K the gear rotation is very fast, a simple two site exchange model describes the amide rotation [21] and the computation times were only 1.5 min and 2 min.

implemented using Java RMI technique. By the parallelization the runtime was decreased considerably (Fig. 9).

4. Example

The program was tested on several molecules. Here the spectra of *N,N*-diisopropyl carbamic acid trimethyl silyl ester (^{i}PrSiC) [20] and that of trimethylsilylcyclopenta-[*l*]-phenantrene ($Me_3Si^{c}PPh$) [18] are shown.

4.1. Temperature dependent spectra of ^{i}PrSiC—a large spin system

The chemical formula of ^{i}PrSiC and its isomerisation reactions are shown on Fig. 10. The possible exchange reactions are the rotation around the amide bond and the simultaneous hindered rotation around the two N–C(^{i}Pr) bonds (gear rotation). The conformational equilibrium of this compound has been studied before and simulations were done for the methine part of the spectra using some simplifications [21]. This time the simulation is done without simplifications so as to show the capability of the algorithm for more complicated systems (without symmetry).

The two parts of ^{1}H NMR spectra of the compound at some temperatures are shown on Figs. 11 and 12 (Bruker AVANCE 250 spectrometer, DMSO-d_6). Above room temperature only one methine signal is present (methyl signal of isopropyl group at 1.08 ppm and methine signal at 3.74 ppm; the trimethyl silyl signal around 0 ppm is not shown). Cooling the sample makes the lines broader and below coalescence temperature two methine signals appear at 3.97 and 4.50 ppm (methyl signals are at 1.07 ppm for both) showing the slowing of rotation around amide bond. These signals get broader again below 280 K and the coalescence of gear rotation occurs around 230 K. After that two rotamers appear with 2:1 molar ratio (see A and B on Fig. 10) and the methine signals of four different isopropyl groups appear at 4.77 (A), 4.62 (B), 2.73 (C) and 2.72 ppm (D) (the last two are overlapping). The signal of ^{i}Pr-methyl groups is divided into four ones as well, their chemical shifts are 1.42, 1.21 and 0.77 ppm (twice). These lines are rather broad due to the viscosity of the solution.

The two isopropyl groups of the molecule—as spin systems—do not interact with each other. It means that simu-

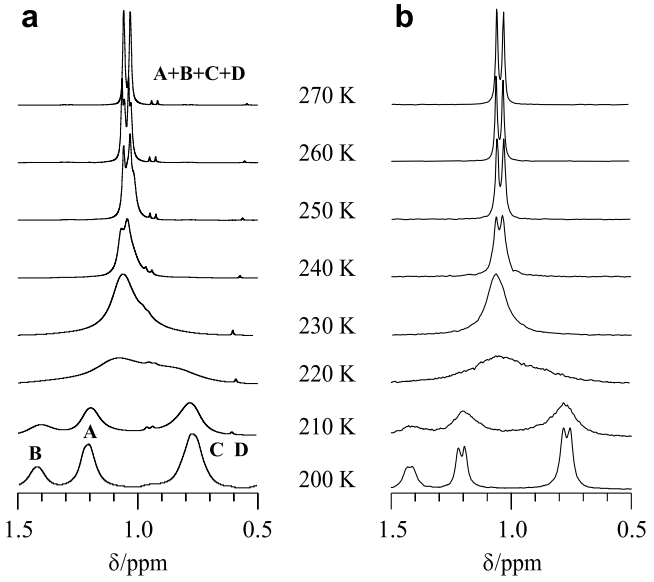

Fig. 12. ^{i}Pr-methyl part of the ^{1}H NMR spectrum of ^{i}PrSiC at different temperatures: (a) Experimental (b) calculated.

Table 1
Chemical shift values used for the simulation of DNMR spectra of ^{i}PrSiC

Sites	δ(CH)/ppm	$\delta(CH_3)$/ppm
A	4.77	1.21
B	4.62	1.43
C	2.73	0.77
D	2.72	0.77

$^{3}J_{H-H} = 7$ Hz.

Table 2
Kinetic coefficient values of amide and gear rotations used for the simulation of DNMR spectra of ^{i}PrSiC at different temperatures

T/K	k_{amide}/s^{-1}	k_{gear}/s^{-1}
200	3.6×10^{-5}	140
210	2.3×10^{-4}	503
220	1.4×10^{-3}	1.6×10^{3}
230	7.7×10^{-3}	4.7×10^{3}
240	3.6×10^{-2}	1.2×10^{4}
250	0.15	3.0×10^{4}
260	0.54	7.0×10^{4}
270	1.8	1.5×10^{5}
280	5.6	3.1×10^{5}
300	43.1	1.1×10^{6}
310	108	2.0×10^{6}
345	1.8×10^{3}	1.2×10^{7}
360	5.1×10^{3}	2.4×10^{7}

Values were calculated from thermodynamic parameters given in text using Eq. (8).

lation can be done for one isopropyl group (seven nuclei) with four possible molecular states (see labelled H and corresponding CH_3 on Fig. 8). With other programs this would mean 4×7 spins ($n=7$ spins and $s=4$ states), and the approximate size of the largest density matrix would be $2\cdot8\cdot s^2\cdot\binom{n}{n/2}^2\cdot\binom{n}{n/2+1}^2 = 16\cdot4^2\cdot\binom{7}{3}^2\cdot\binom{7}{4}^2 = 0.4$ Gbyte with all possible simplifications except symmetry. With our new method the required RAM is only $8\cdot\binom{n}{n/2}^2 = 8\cdot\binom{7}{3}^2 = 9.6$ Kbyte.

Spectral data used for simulation are shown in Table 1. The slight temperature dependence of the chemical shifts was neglected. The methyne and ^{i}Pr-methyl part of spectra were simulated independently (this is only important because of resolution). The following thermodynamic data were used: $\Delta S^{++} = 15.0$ J K^{-1} mol^{-1} and $\Delta H^{++} = 68.6$ kJ mol^{-1} for amide rotation and $\Delta S^{++} = 14.0$ J K^{-1} mol^{-1} and $\Delta H^{++} = 42.9$ kJ mol^{-1} for the gear rotation [22]. Calculated kinetic coefficients at different temperatures are shown in Table 2. The number of spectrum points was 512 and simulations were done with 100 scans. As it is seen on Figs. 11 and 12 the experimental and calculated curves are fitting well.

4.2. Temperature dependent spectra of $Me_3{}^{c}PPh$—a strongly coupled spin system

The chemical formula of $Me_3{}^{c}PPh$ is shown on Fig. 13. The process in question is the migration of the Me_3Si group from C^1 to C^3. This mutual exchange reaction was studied earlier by dynamic NMR and EXSY measurements [23] and the measured thermodynamic data were $\Delta H^{++} = 63.6$ kJ mol^{-1} and $\Delta S^{++} = 34.3$ J K^{-1} mol^{-1}.

Here the spectra of the eight spin system H^4 to H^{11} were simulated at five different temperatures (Fig. 14). Spectroscopic parameters used for the simulation are shown in Table 3. The spin system H^4 to H^7 is uncoupled to other protons therefore the system can be simulated as four spins in two states: where the Me_3Si is at position 1 and at 3.

5. Conclusions

The program presented is based on the vector model combined with Monte Carlo simulations. The vector model was extended to coupled spin systems and the behaviour of base functions are determined calculating with their discrete frequency distribution.

The main advantage of the MC-DNMR program is that it deals with significantly smaller matrices than the methods based on the calculation of the density matrix. Therefore larger spin systems can be handled with it than any other simulation program earlier. The runtime is nearly independent of the number of conformers which makes it very useful in the case of non-mutual exchanges with many possible sites.

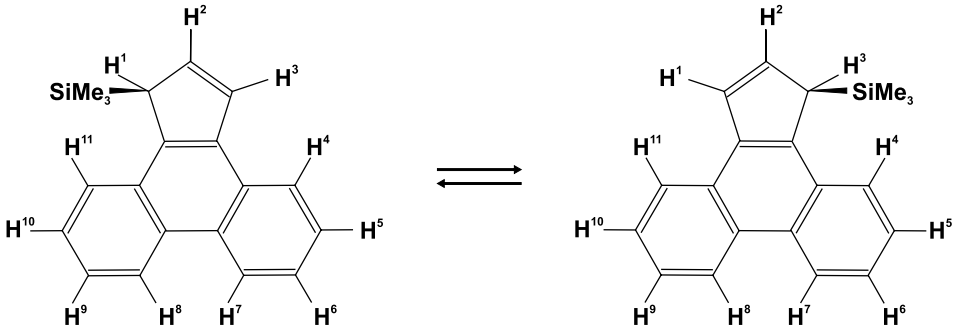

Fig. 13. Structure and numbering of $Me_3{}^{c}PPh$.

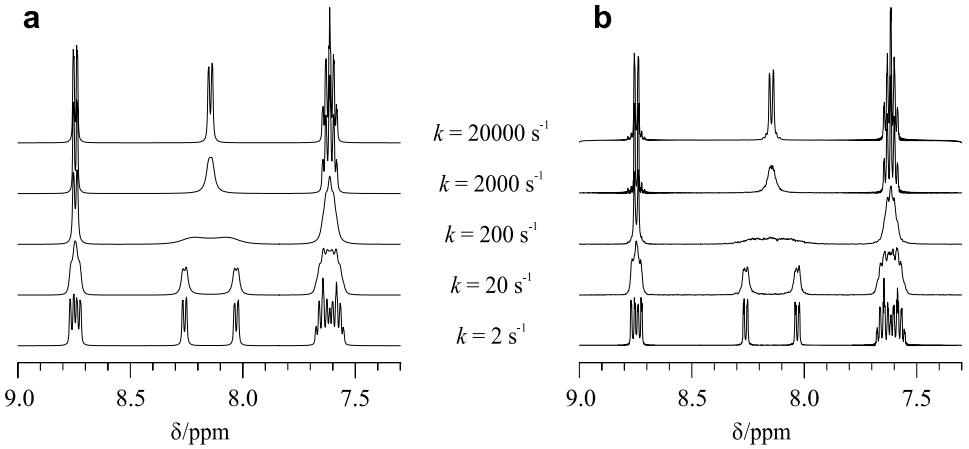

Fig. 14. Simulated temperature dependent spectra of $Me_3{}^cPPh$ (a) MEXICO (b) MC-DNMR. The simulation of the spectra (SI = 1024, NS = 1000 scans) with MC-DNMR program was performed with 16 Java threads on four nodes of an FSC Primergy Server, each node with two 1.8 GHz AMD Opteron dual-core processors. The computation times were 33, 35, 48, 133 and 990 s for $k = 2$, 20, 200, 2000 and 20,000 s^{-1}, respectively. The same calculation was done on a desktop PC with Intel Core-2 Duo 2.66 GHz processor and Windows XP operating system using two Java threads. The computation times were 1, 1, 1.2, 3.5 and 25 min for the same k series.

Table 3
Chemical shift values (δ in ppm) and coupling constants (J in Hz) used for the simulation of DNMR spectra of $Me_3Si{}^cPPh$ [23]

	State 1	State 2
δ_4	8.26	8.03
δ_5	7.66	7.60
δ_6	7.63	7.57
δ_7	8.76	8.73
J_{45}	8.3	8.3
J_{46}	1.5	1.8
J_{47}	0.5	0.6
J_{56}	6.8	6.7
J_{57}	1.5	1.8
J_{67}	8.3	8.3

Acknowledgments

We thank Dr. E. Rohonczy-Boksay for her useful comments, Dr. Ö. Farkas at Eötvös Loránd University and Dr. Gy. Dombi at the University of Szeged, Hungary for their support at testing the program in multiprocessor environment.

References

[1] A.E. Derome, Modern NMR Techniques for Chemistry Research, Pergamon Press, Oxford, 1993.
[2] J. Sandstrom, Dynamic NMR Spectroscopy, Academic Press, London, 1982.
[3] J.K.M. Sanders, B.K. Hunter, Modern NMR Spectroscopy, Oxford Univ. Press, Oxford, 1993.
[4] R.R. Ernst, G. Bodenhausen, A. Wokaun, Principles of Nuclear Magnetic Resonance in One and Two Dimensions, Clarendon Press, Oxford, 1987.
[5] L.M. Jackman, F.A. Cotton, Dynamic Nuclear Magnetic Resonance Spectroscopy;, Academic Press, New York, 1975.
[6] J.I. Kaplan, G. Fraenkel, NMR of Chemically Exchanging Systems, Academic Press, New York, 1980.
[7] J.W. Emsley, J. Feeney, L.H. Sutcliffe, High Resolution NMR Spectroscopy, Pergamon Press, New York, 1965.
[8] G. Binsch, A unified theory of exchange effects on nuclear magnetic resonance line shapes, J. Am. Chem. Soc. 91 (1969) 1304–1309.
[9] D.A. Kleier, G. Binsch, General theory of exchange-broadened NMR line shapes II. Exploitation of invariance properties, J. Magn. Reson. 3 (1970) 146–160.
[10] D.S. Stephenson, G. Binsch, Iterative computer analysis of complex exchange-broadened NMR bandshapes, J. Magn. Reson. 32 (1978) 145–152.
[11] S. Szymanski, G. Binsch, A Liouville space formulation of Wangsness–Bloch–Redfield theory of nuclear spin relaxation II. Scalar relaxation, J. Magn. Reson. 81 (1989) 104–120.
[12] A.D. Bain, G.J. Duns, A new approach to the calculation of NMR lineshapes of exchanging systems, J. Magn. Reson. A 112 (1995) 258–260.
[13] A.D. Bain, G.J. Duns, A unified approach to dynamic NMR based on a physical interpretation of the transition probability, Can. J. Chem. 74 (1996) 819–824.
[14] A.D. Bain, D.M. Rex, R.N. Smith, Fitting dynamic NMR lineshapes, Magn. Reson. Chem. 39 (2001) 122–126.
[15] H.J. Reich, W.S. Goldenberg, B.Ö. Gudmundsson, A.W. Sanders, K.J. Kulicke, S. Simon, I.A. Guzei, Amine-chelated Aryllithium reagents-structure and dynamics, J. Am. Chem. Soc. 123 (2001) 8067–8079.
[16] H.J. Reich, J. Chem. Educ. Software 3D2 (1996).
[17] http://www.bruker-biospin.com/topspin_structure_analysis.html.
[18] R.S. Dumont, S. Jain, A.D. Bain, Simulation of many-spin system dynamics via sparse matrix methodology, J. Chem. Phys. 106 (1997) 5928–5936.
[19] R.S. Dumont, P. Hazendouk, A.D. Bain, Dual Lanczos simulation of dynamic nuclear magnetic resonance spectra for systems with many spins or exchange sites, J. Chem. Phys. 113 (2000) 3270–3281.
[20] J. Rohonczy, D. Knausz, B. Csákvári, P. Sohár, I. Pelczer, L. Párkányi, Trimethylsilylated *N*-alkyl-substituted carbamates III. Structure of trimethylsilyl-*N,N*-diisopropyl carbamate in solid phase and in solution, J. Orgmet. Chem. 340 (1988) 293–302.
[21] Bruker TopSpin DNMR module manual.
[22] J. Rohonczy, Total lineshape analysis of DNMR spectra by IBM personal computer, Kem. Kozl. 74 (1992) 161–200.
[23] S.S. Rigby, H.K. Gupta, N.H. Werstiuk, A.D. Bain, M.J. McGlinchey, Do aromatic transition states lower barriers to silantropic shifts? A synthetic, NMR spectroscopic and computational study, Inorg. Chim. Acta 251 (1996) 355–364.